Journal of Agrometeorology

(A publication of Association of Agrometeorologists)

ISSN : 0972-1665 (print), 2583-2980 (online)
Vol. No. 28 (2) : 269-273 (June - 2026)
https://doi.org/10.54386/jam.v28i1.3276
https://journal.agrimetassociation.org/index.php/jam

Short communication

Fusion of Multispectral and Microwave Sensor Data for Monitoring Land Surface Temperature in Agro-Meteorological Studies

MAHESH PALAKURU[*1], SURYA PRAKASH REDDY M.[1], ASHWINI KUMAR[2], SUNDAR BORKAR[3], JAWAHARLAL D.[4], SAI KUMAR R.[4], SUDHARSHANA C.[5] and BABY Y.[6]

[1]School of Agricultural Sciences, Malla Reddy University, Hyderabad-500100, Telangana, India
[2]RAK College of Agriculture, Sehore, Madhya Pradesh, India
[3]Bhaganthrao Mandloi College of Agriculture, Ramnagar, Khandwa-450001, Madhya Pradesh, India
[4]Professor Jayashankar Telangana Agricultural University, Rajendranagar, Hyderabad-500030, India,
[5]College of Agriculture, Annamacharya University, Rajampeta-516126, Andhra Pradesh, India
[6]Annamacharya Institute of Technology & Sciences, Venkatapuram, Renigunta- 517520, Tirupati, Chitoor District, Andhra Pradesh, India
[*]Communication author email: pmahesh89@gmail.com

This study presents an exploratory comparison of Land Surface Temperature (LST) derived from Landsat-8 Band 10 thermal infrared (TIR, 30 m) and SCATSAT-1 Ku-band microwave brightness temperature (BT, 2.2 km) over Tirupati district, Andhra Pradesh, India. LST was retrieved using an eight-step mono-window algorithm (Equations 1–8). SCATSAT-1 data were resampled to 30 m via bilinear interpolation prior to comparison. At 404 co-located sampling points, mean LST was 35.1°C (Landsat-8) and 31.2°C (SCATSAT-1), with a systematic cool bias of −3.93°C, RMSE = 5.38°C, MAE = 4.65°C, and R^2 = 0.003. The low R^2 reflects the inherent spatial resolution mismatch between sensors rather than sensor failure. Results demonstrate the all-weather potential of SCATSAT-1 for LST monitoring while identifying spatial downscaling and in-situ validation as priority needs for future multi-sensor fusion work.

Land Surface Temperature (LST) is a fundamental parameter of surface energy balance, agro-meteorological monitoring, and climate variability (Li *et al.,* 2013; Jiménez-Muñoz *et al.,* 2014). Conventional ground instruments are incapable of providing the spatial coverage needed for regional agricultural management; remote sensing therefore offers the only practical means of large-scale LST estimation (Anderson *et al.,* 2016; Karnieli *et al.,* 2018). Landsat-8 carries the Thermal Infrared Sensor (TIRS), providing TIR-based LST at 30 m resolution. SCATSAT-1, a Ku-band (13.515 GHz) scatterometer operated by ISRO, provides passive microwave BT at ~2.2 km resolution under all-weather conditions—a significant operational advantage over TIR sensors in cloud-affected monsoon regions (Kumar *et al.,* 2022; Mohanty *et al.*, 2021). Although optical–microwave data fusion has been explored for soil moisture and land cover (Dash *et al.,* 2023; Du *et al.,* 2020), a methodologically transparent comparison of Landsat-8 TIR and SCATSAT-1 Ku-band LST, with explicit treatment of spatial resolution mismatch and statistical uncertainty, has not been reported for Indian agro-climatic regions. This study addresses that gap.

The study was conducted over Tirupati district (8,229 km²; 13°20′N–14°15′N, 78°55′E–80°02′E), Andhra Pradesh, India (Fig. 1). The district has a tropical monsoon climate (annual rainfall 900–1,000 mm, summer maxima up to 42°C) with sandy clay loam soils (55%) supporting groundnut, irrigated paddy, and double-cropping systems—conditions representative of agronomically diverse semi-arid environments suitable for evaluating LST variability (Palakuru & Yarrakula, 2019). Contemporaneous Landsat-8 and SCATSAT-1 data acquired on 25 February 2020 were used (Table 1).

A fundamental challenge is the spatial resolution mismatch: each SCATSAT-1 pixel integrates surface information over an area ~5,382 times larger than a Landsat-8 pixel. To enable pixel-level comparison, SCATSAT-1 BT was resampled to 30 m using bilinear interpolation in ArcGIS 10.8. This resampling creates no genuine spatial detail at 30 m; the spatial information content of SCATSAT-1 remains constrained to its native 2.2 km footprint.

Article info - DOI: *https://doi.org/10.54386/jam.v28i1.3276*
Received: 27 November 2025; Accepted: 06 May 2026; Published online : 04 June 2026

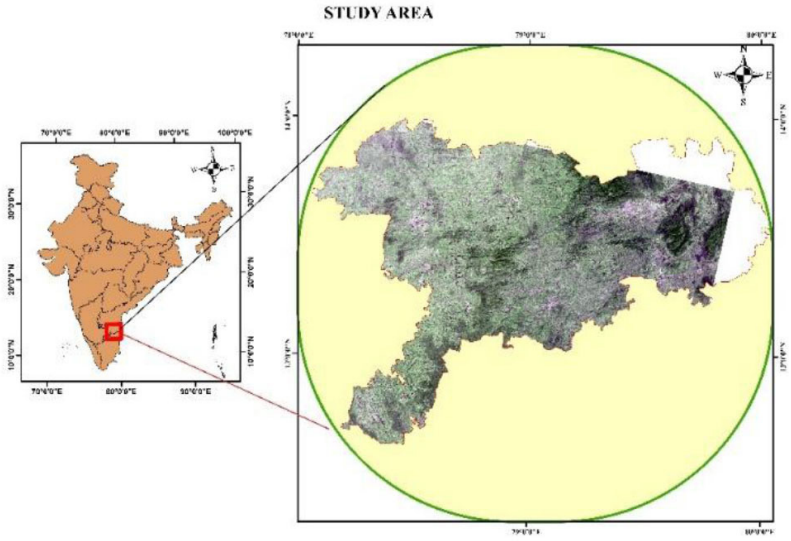

Fig. 1: Study area: Tirupati district, Andhra Pradesh, India.

Table 1: Satellite data properties

Parameter	Landsat-8	SCATSAT-1
Band / Channel	Band 10 (TIR)	Ku-band (HH/HV)
Spatial resolution	30 m	2.2 km
Date of acquisition	25 February 2020	25 February 2020
Sensor type	Multispectral / TIR	Microwave scatterometer
Product type	Level-1 ToA radiance	Brightness temperature
Data source	USGS Earth Explorer	MOSDAC, ISRO

This disparity is the primary cause of the low pixel-level correlation observed ($R^2 = 0.003$) and must not be construed as sensor invalidity. Future studies should apply physically-based disaggregation (e.g., DisTrad, machine-learning super-resolution) before operational fusion.

LST was retrieved following an eight-step procedure. (i) ToA spectral radiance ($L\lambda$, $W \cdot m^{-2} \cdot sr^{-1} \cdot \mu m^{-1}$) was computed from Landsat-8 Band 10 digital numbers (Wang *et al.,* 2015):

$$L\lambda = M_L \times Qcal + A_L \quad (1)$$

M_L = multiplicative scaling factor; A_L = additive scaling factor; Qcal = calibrated DN (from MTL metadata).

(ii) At-sensor brightness temperature BT (K) was derived from $L\lambda$ using Band 10 calibration constants (Li *et al.,* 2013):

$$BT = K_2 / \ln(K_1 / L\lambda + 1) \quad (2)$$

$K_1 = 774.89\ W \cdot m^{-2} \cdot sr^{-1} \mu m^{-1}$; $K_2 = 1{,}321.08$ K (Landsat-8 Band 10, MTL metadata). BT converted to °C by subtracting 273.15.

(iii) NDVI was calculated from Bands 5 (NIR) and 4 (Red) (Rozenstein *et al.,* 2019):

$$NDVI = (B_5 - B_4) / (B_5 + B_4) \quad (3)$$

(iv) Fractional vegetation proportion (Pv) was estimated as (Rozenstein *et al.*, 2019):

$$Pv = [(NDVI - NDVImin) / (NDVImax - NDVImin)]^2 \quad (4)$$

(v) Land surface emissivity (ε) was computed via the NDVI threshold method (Rozenstein *et al.,* 2019):

$$\varepsilon = \varepsilon v \times Pv + \varepsilon s \times (1 - Pv) + d\varepsilon \quad (5)$$

$\varepsilon v = 0.986$; $\varepsilon s = 0.966$; $d\varepsilon = 4 \times (1 - \varepsilon s) \times \varepsilon v \times Pv \times (1 - Pv) \times 0.55$. Emissivity ranged 0.96–0.99.

(vi) LST from Landsat-8 was retrieved by the mono-window Planck-based inversion (Jiménez-Muñoz *et al.,* 2014):

$$LST\_L8 = BT / [1 + (\lambda \times BT / \rho) \times \ln(\varepsilon)] \quad (6)$$

$\lambda = 10.895$ μm (Band 10 effective wavelength); $\rho = 1.438 \times 10^{-2}$ m·K. Output in K; converted to °C.

(vii) SCATSAT-1 raw backscatter was converted to sigma-naught (σ°, dB) (Rozenstein *et al.,* 2019):

$$\sigma^\circ\ (dB) = 10 \times \log_{10} (\sigma^\circ\ linear) \quad (7)$$

(viii) LST from SCATSAT-1 was derived from its Ku-band BT

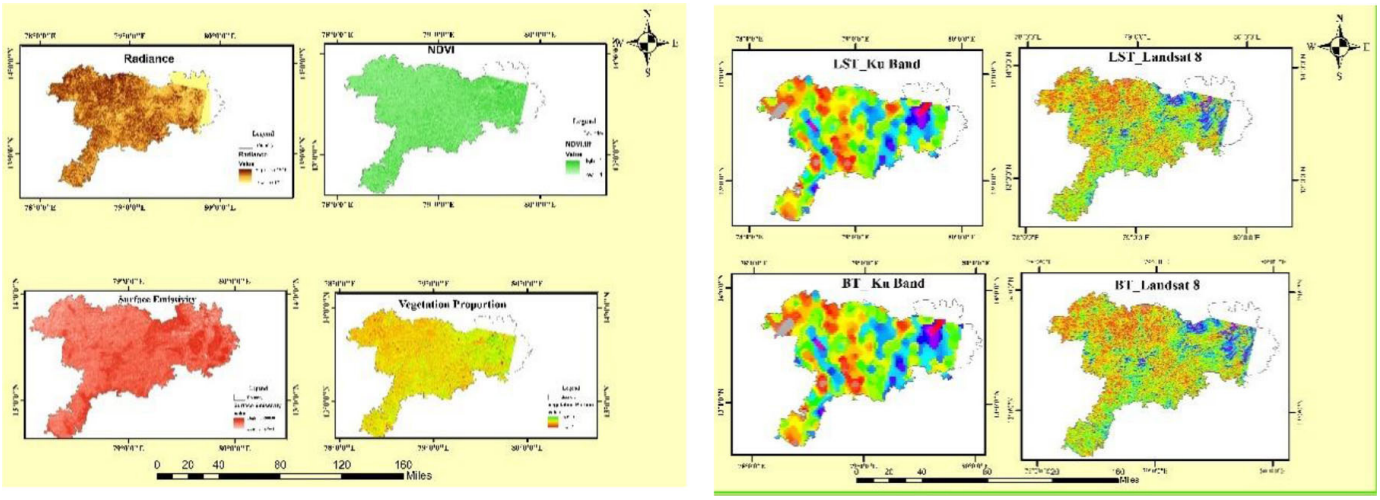

Fig. 2: Spatial maps: NDVI, radiance, emissivity, Pv, BT and LST from both sensors

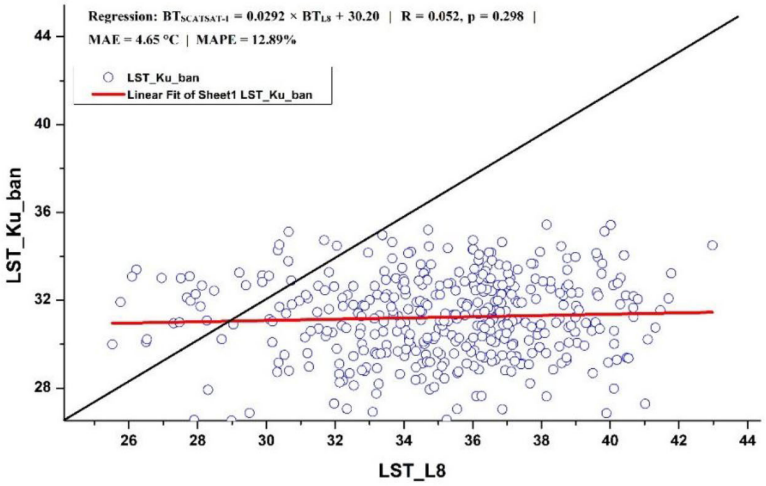

Fig. 3: Scatter plot: SCATSAT-1 BT vs. Landsat-8 BT at 404 sampling points

(resampled to 30 m) using the same Planck inversion (Mohanty *et al.,* 2021):

$$LST\_SCAT = BT\_ku / [1 + (\lambda p \times BT\_ku / \rho) \times ln(\varepsilon)] \quad (8)$$

Where, λp = equivalent wavelength for 13.515 GHz Ku-band (≈ 22.2 mm); ε from Eq. 5. This Planck inversion approximation for active microwave data is an acknowledged limitation requiring further empirical evaluation.

Accuracy assessment was performed at 404 co-located points (systematic fishnet grid, ArcGIS 10.8). Metrics included R^2, Pearson R, RMSE, MBE, MAE, and MAPE. No in-situ ground-based LST measurements were available; all statistics therefore reflect inter-sensor agreement rather than absolute accuracy. Future studies must incorporate calibrated radiometric observations (automatic weather stations, flux towers, handheld infrared thermometers) to independently validate both products.

The Landsat-8 processing chain yielded spectral radiance in the range −0.19 to 15.45 $W \cdot m^{-2} \cdot sr^{-1} \mu m^{-1}$, NDVI from 0 to 1, vegetation proportion from 0 to 1, and emissivity from 0.96 to 0.99, consistent with mixed agricultural surfaces. BT from Landsat-8 ranged from 26°C to 41°C, capturing fine-scale thermal heterogeneity across soil, canopy, and irrigated land. BT from SCATSAT-1 Ku-band ranged from 24°C to 32°C—a narrower range attributable to spatial averaging over its coarse 2.2 km footprint. Unlike TIR sensors, SCATSAT-1 can acquire data under cloudy conditions, offering an operational advantage during monsoon seasons (Palakuru *et al.,* 2020). Spatial distributions of all parameters are illustrated in Fig. 2.

Mean LST from Landsat-8 was 35.1°C and from SCATSAT-1 was 31.2°C. Inter-sensor comparison at 404 points revealed a systematic cool bias of −3.93°C in SCATSAT-1 (Table 2; Fig. 3). The regression of SCATSAT-1 BT on Landsat-8 BT yielded BTSCAT = 0.0292 × BTL8 + 30.20 (R = 0.052, p = 0.298), confirming the absence of a statistically significant linear relationship at the pixel scale. The near-zero slope and R^2 = 0.003

Table 2: Statistical metrics from inter-sensor LST comparison (n = 404)

Metric	Value	Interpretation
Mean LST: Landsat-8 (°C)	35.10	Mean over 404 sampling points
Mean LST: SCATSAT-1 (°C)	31.20	After bilinear resampling to 30 m
MBE (°C)	−3.93	Systematic cool bias in SCATSAT-1
RMSE (°C)	5.38	Root mean square inter-sensor deviation
MAE (°C)	4.65	Mean absolute difference
MAPE (%)	12.89	Mean absolute percentage error
R^2	0.003	Negligible pixel-level correlation; due to resolution mismatch
Pearson R (p-value)	0.052 (0.298)	Not statistically significant at $\alpha = 0.05$

are predictable consequences of comparing a 30 m TIR product with a spatially downscaled 2.2 km microwave product: sub-field-scale thermal variability captured by Landsat-8 (soil patches, irrigation channels, crop rows) is entirely smoothed within SCATSAT-1's coarse footprint. The MBE (−3.93°C) is the more diagnostic metric, reflecting a systematic sensor offset arising from radiometric, wavelength-dependent, and resolution differences. Inter-sensor biases of 2–5°C between TIR and microwave LST products are well-documented in the literature (Du *et al.,* 2020; Dash *et al.,* 2023), and our findings fall within that expected range.

To improve multi-sensor LST fusion accuracy, future studies should: (1) apply physically-based spatial downscaling (DisTrad, NDVI-assisted regression, or deep-learning super-resolution) to disaggregate SCATSAT-1 BT before comparison; (2) incorporate in-situ LST validation from calibrated radiometers or automatic weather stations; (3) implement atmospheric correction via radiative transfer modelling or a split-window algorithm to address water vapour effects differentially affecting TIR and microwave retrievals; (4) develop a unified joint-retrieval framework that integrates both sensor BT streams within a single physically-based model, rather than independently computing LST and post-hoc comparing; and (5) extend analysis to multi-temporal datasets across crop growth stages to capture seasonal LST dynamics relevant to agro-meteorological applications.

In summary, this study demonstrates that SCATSAT-1 Ku-band data can retrieve LST values broadly consistent with Landsat-8 TIR estimates (mean difference 3.93°C), while providing an all-weather observational capability that TIR sensors cannot match. The weak pixel-level correlation ($R^2 = 0.003$) is primarily a scale artefact of the 30 m vs. 2.2 km resolution disparity, and the absence of in-situ ground-truth measurements limits absolute validation. These findings establish a baseline for future multi-sensor LST fusion over Indian agro-climatic regions and highlight the methodological steps—spatial downscaling, atmospheric correction, and ground-truth validation—needed to operationalize such fusion products for precision agro-meteorology.

ACKNOWLEDGEMENTS

The authors gratefully acknowledge the USGS for providing Landsat-8 data and ISRO/MOSDAC for providing SCATSAT-1 data.

Author's certificate: The manuscript or its part is not under consideration for publication elsewhere and the same has been approved by all co-authors.

Conflict of Interests: The authors declare that there is no conflict of interest regarding the publication of this article.

Funding: This research received no external funding. The study was carried out as part of the academic research activities of the authors' institutions.

Authors contribution: **Mahesh Palakuru:** Conceptualisation, Methodology, Writing (Original draft); **Surya Prakash Reddy M:** Data Acquisition, Processing; **Aswini Kumar:** Validation, Formal Analysis; **Sundar Borkar:** Data Curation, Software; **Jawaharlal D.:** Investigation; **Sai Kumar R.:** Visualisation; **Sudharsana C.:** Review and Editing; **Baby Y.:** Review And Editing.

Disclaimer: The contents, opinions, and views expressed in the research article published in the Journal of Agrometeorology are the views of the authors and do not necessarily reflect the views of the organisations they belong to.

Publisher's Note: The periodical remains neutral concerning jurisdictional claims in published maps and institutional affiliations.

REFERENCES

Anderson, M. C., Allen, R. G., Morse, A., & Kustas, W. P. (2016). Agro-meteorological applications of fused land surface temperature data. *Agricultural and Forest Meteorology, 216*, 1–15. https://doi.org/10.1016/j.agrformet.2015.10.002

Dash, P., Lanza, L. G., & Fox, N. T. (2023). Emissivity correction in microwave–optical fusion for land surface temperature estimation. *International Journal of Remote Sensing, 44*(5), 1234–1256.

Du, C., Ren, H., Qin, Q., & Li, Z. L. (2020). Microwave land surface temperature estimation using Ku-band polarimetric observations. *IEEE Transactions on Geoscience and Remote Sensing, 58*(7), 4567–4578. https://doi.org/10.1109/TGRS.2019.2960123

Jiménez-Muñoz, J. C., Sobrino, J. A., Skoković, D., & Mattar, C. (2014). Land surface temperature retrieval methods from

Landsat-8 thermal infrared sensor data. *IEEE Geoscience and Remote Sensing Letters, 11*(10), 1840–1843. https://doi.org/10.1109/LGRS.2014.2312032

Karnieli, A., Agam, N., Pinker, R. T., Atlas, R., Bayarjargal, Y., Berk, Y., et al. (2018). Use of NDVI and land surface temperature for drought assessment. *Remote Sensing, 10*(12), 1885. https://doi.org/10.3390/rs10121885

Kumar, A., Singh, R. P., & Patel, N. R. (2022). SCATSAT-1 applications for land surface monitoring in monsoon-dominated regions. *Current Science, 122*(5), 567–575.

Li, Z. L., Tang, B. H., Wu, H., Ren, H., Yan, G., Wan, Z., et al. (2013). Satellite-derived land surface temperature: Current status and perspectives. *Remote Sensing of Environment, 131*, 14–37. https://doi.org/10.1016/j.rse.2012.12.008

Mohanty, S., Patel, N. R., & Rathore, V. S. (2021). Fusion of Ku-band scatterometer and optical data for agricultural applications. *ISPRS Journal of Photogrammetry and Remote Sensing, 175*, 45–60. https://doi.org/10.1016/j.isprsjprs.2021.02.012

Palakuru, M., & Yarrakula, K. (2019). Study on paddy phenomics ecosystem and yield estimation using space-borne multi-sensor remote sensing data. *Journal of Agrometeorology, 21*(2), 115–123.

Palakuru, M., Adamala, S., & Debnath, S. (2020). Application of traditional irrigation systems for sustainable agriculture in India. *International Journal of Modern Agriculture, 9*(4), 12–22.

Rozenstein, O., Zhao, W., & Dash, J. (2019). Use of SCATSAT-1 sigma-0 for soil moisture and land surface temperature estimation. *IEEE Journal of Selected Topics in Applied Earth Observations and Remote Sensing, 12*(9), 3456–3467. https://doi.org/10.1109/JSTARS.2019.2924538

Sobrino, J. A., Li, Z. L., & Romaguera, M. (2019). Split-window algorithm for land surface temperature retrieval from Landsat-8 data. *Remote Sensing of Environment, 225*, 1–12. https://doi.org/10.1016/j.rse.2019.02.017

Wang, F., Qin, Z., Song, X., Zhou, H., & Xiao, W. (2015). An improved mono-window algorithm for land surface temperature retrieval from Landsat-8 TIRS. *Remote Sensing, 7*(9), 11244–11263. https://doi.org/10.3390/rs70911244